HHS Public Access

Author manuscript

Cell Rep. Author manuscript; available in PMC 2021 July 29.

Published in final edited form as:

Cell Rep. 2021 July 06; 36(1): 109309. doi:10.1016/j.celrep.2021.109309.

Integrin αvβ8 on T cells suppresses anti-tumor immunity in multiple models and is a promising target for tumor immunotherapy

Eswari Dodagatta-Marri[1,10], **Hsiao-Yen Ma**[2,10], **Benjia Liang**[2,3], **John Li**[2], **Dominique S. Meyer**[1], **Szu-Ying Chen**[1], **Kai-Hui Sun**[2], **Xin Ren**[2], **Bahar Zivak**[4], **Michael D. Rosenblum**[4], **Mark B. Headley**[5], **Lauren Pinzas**[1], **Nilgun I. Reed**[2], **Joselyn S. Del Cid**[2], **Byron C. Hann**[1], **Sharon Yang**[6], **Anand Giddabasappa**[7], **Kavon Noorbehesht**[7], **Bing Yang**[7], **Joseph Dal Porto**[8], **Tatsuya Tsukui**[2], **Kyle Niessen**[8,11,12], **Amha Atakilit**[2,11,12], **Rosemary J. Akhurst**[1,9,11,12,*], **Dean Sheppard**[2,11,12,13,*]

[1]Helen Diller Family Comprehensive Cancer Center, University of California, San Francisco, San Francisco, CA, USA

[2]Lung Biology Center, Department of Medicine, University of California, San Francisco, San Francisco, CA, USA

[3]Department of Gastrointestinal Surgery, Shandong Provincial Hospital Affiliated to Shandong University, Jinan 250021, Shandong, China

[4]Department of Dermatology, University of California, San Francisco, San Francisco, CA, USA

[5]Department of Pathology, University of California, San Francisco, San Francisco, CA, USA

[6]Comparative Medicine, Pfizer Inc., San Diego, CA, USA

[7]Oncology Research Unit, Pfizer Inc., Pearl River, NY, USA

[8]Pfizer Centers for Therapeutic Innovation, San Francisco, CA, USA

[9]Department of Anatomy, University of California, San Francisco, San Francisco, CA, USA

[10]These authors contributed equally

[11]These authors contributed equally

[12]Senior author

[*]Correspondence: rosemary.akhurst@ucsf.edu (R.J.A.), dean.sheppard@ucsf.edu (D.S.).

AUTHOR CONTRIBUTIONS

E.D.-M. and H.-Y.M. wrote the manuscript and designed and performed experiments. B.L. and J.L. designed and performed experiments and oversaw immunophenotyping. D.S.M. and B.C.H. developed the CCK168 tumor cell line model and performed *in vivo* tumor experiments. K.-H.S., X.R., N.I.R., J.S.D.C., and T.T. performed ADWA-11 antibody characterization experiments and designed, performed, and interpreted immunostaining experiments and *in vivo* tumor experiments. B.Z., M.D.R., and M.B.H. performed mouse immunophenotyping experiments. S.-Y.C., A.G., K. Niessen, B.Y., K. Noorbehesht, and J.D.P. developed the effectorless ADWA-11 antibody, performed *in vivo* tumor experiments using the effectorless ADWA-11 antibody, and analyzed data. A.A. developed the ADWA-11 antibody and designed and performed experiments. K. Niessen, R.J.A., and D.S. wrote and edited the manuscript, designed experiments, analyzed data, and oversaw all aspects of the work. The authors acknowledge assistance from Maeva Adoumie with immunophenotyping.

SUPPLEMENTAL INFORMATION

Supplemental information can be found online at https://doi.org/10.1016/j.celrep.2021.109309.

[13]Lead contact

SUMMARY

αvβ8 integrin, a key activator of transforming growth factor β (TGF-β), inhibits anti-tumor immunity. We show that a potent blocking monoclonal antibody against αvβ8 (ADWA-11) causes growth suppression or complete regression in syngeneic models of squamous cell carcinoma, mammary cancer, colon cancer, and prostate cancer, especially when combined with other immunomodulators or radiotherapy. αvβ8 is expressed at the highest levels in CD4+CD25+ T cells in tumors, and specific deletion of β8 from T cells is as effective as ADWA-11 in suppressing tumor growth. ADWA-11 increases expression of a suite of genes in tumor-infiltrating CD8+ T cells normally inhibited by TGF-β and involved in tumor cell killing, including granzyme B and interferon-γ. The *in vitro* cytotoxic effect of tumor CD8 T cells is inhibited by CD4+CD25+ cells, and this suppressive effect is blocked by ADWA-11. These findings solidify αvβ8 integrin as a promising target for cancer immunotherapy.

Graphical abstract

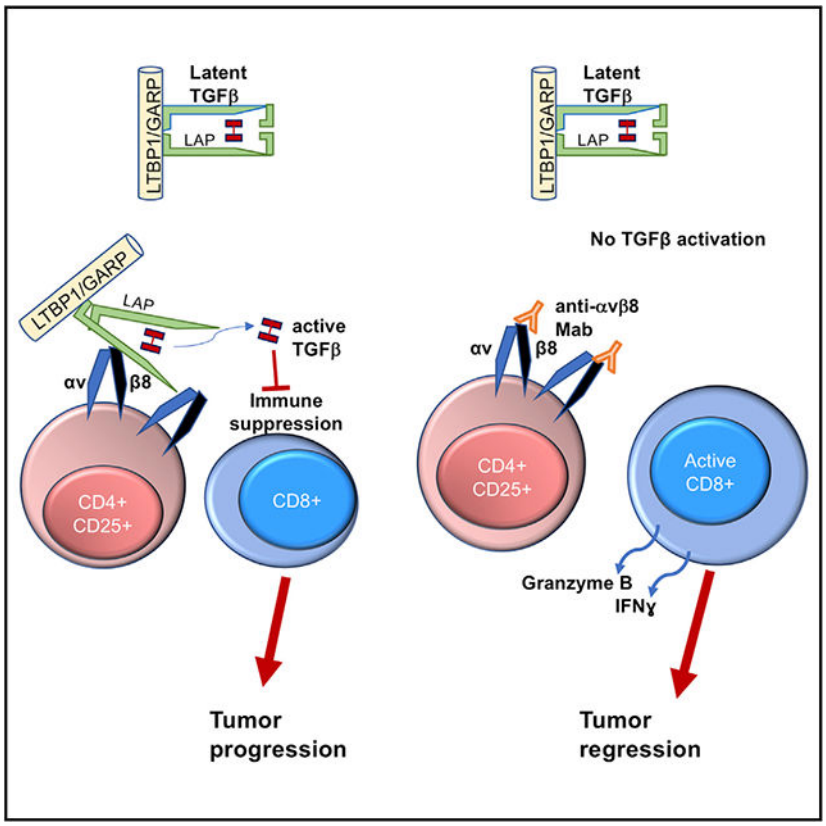

In brief

TGF-β suppresses anti-tumor immunity. Dodagatta-Marri, Ma et al. show that the TGF-β-activating integrin αvβ8 is expressed on CD25+CD4+ tumor T cells and suppresses anti-tumor immunity by CD8+ T cells. Blocking this integrin enhances tumor cell killing and synergizes with multiple immune modulators or radiotherapy to induce long-term anti-tumor immunity.

INTRODUCTION

Immune checkpoint inhibitors have revolutionized treatment of cancer by allowing host adaptive immunity to eliminate tumor cells. For example, antibodies targeting the immune checkpoint PD-1 or its ligand PD-L1 can induce persistent anti-tumor immunity and have become standard therapies for melanoma, lung cancer, head and neck cancers, renal cell carcinoma, and bladder cancer (Sharma and Allison, 2015). However, only a minority of affected individuals benefit from these treatments. Therefore, intense efforts are underway to develop additional immunomodulatory strategies to extend the reach of this exciting new approach to treating cancer.

Transforming growth factor β (TGF-β) is a potent suppressor of adaptive immunity and an important mediator of immune suppression by a subset of regulatory T cells (Gorelik and Flavell, 2001). TGF-β also promotes secretion and accumulation of a fibrotic tumor stroma that has been proposed as a possible contributor to exclusion of immune cells from some solid tumors. For all of these reasons, inhibition of TGF-β has been widely explored as an adjunctive immunotherapy (Derynck et al., 2021).

Previous studies have shown that inhibition of TGF-β signaling can enhance responses to checkpoint inhibitors (Dodagatta-Marri et al., 2019; Mariathasan et al., 2018; Tauriello et al., 2018). However, TGF-β plays important homeostatic roles in many biological systems, so effective systemic targeting of TGF-β signaling would likely present challenges because of un-wanted side effects (Akhurst and Hata, 2012; Flavell et al., 2010). Strategies that limit inhibition of TGF-β to specific biological contexts, especially those that contribute to suppression of tumor immunity, could have significant safety and therapeutic advantages over systemic TGF-β inhibition. One such strategy takes advantage of the role of specific integrin receptors in activating TGF-β because integrins can only activate TGF-β1 and TGF-β3, and integrins are restricted in where and when they perform this function. Blockade of integrin by circumventing inhibition of TGF-β2 homodimers may be advantageous for avoiding possible outgrowth of dormant metastatic tumor cells that are growth inhibited by TGF-β2 in bone and lymph nodes (Bragado et al., 2013; Jiang et al., 2019; Yumoto et al., 2016).

One previous study showed that an antibody against αvβ8 could inhibit growth of syngeneic tumors in mice, and that study suggested that antibody blockade acted principally on αvβ8 expressed on tumor cells (Takasaka et al., 2018). In the current study, we utilized a potent αvβ8-blocking monoclonal antibody (ADWA-11) we had generated previously by immunizing *Itgb8* knockout mice with recombinant αvβ8 (Stockis et al., 2017) to examine whether and how inhibition of this integrin could facilitate anti-tumor immunity. This antibody was highly potent in inhibiting αvβ8-mediated TGF-β activation in a co-culture bioassay system, and we found that it potently inhibited growth of tumors irrespective of the level of αvβ8 on tumor cells. All responding tumor types showed the highest levels of *Itgb8* expression in CD25+ CD4+ T cells. Deletion of *Itgb8* specifically in T cells was as effective in suppressing tumor growth as ADWA-11, and ADWA-11 treatment did not further inhibit tumor growth in mice lacking *Itgb8* in T cells. These results are consistent with the idea that

inhibition of αvβ8 enhances anti-tumor immunity, at least in part, by blocking αvβ8-mediated TGF-β activation by T cells and suggest that inhibition of this integrin could be a promising therapeutic strategy for a wide array of tumors.

RESULTS

Effects of combination therapy of ADWA-11 and anti-PD-1 in CCK168 squamous cell, EMT6 mammary, and TRAMPC2 prostate carcinoma models

We began by examining the effects of ADWA-11 alone or in combination with anti-PD-1 in established syngeneic tumor models of squamous cell carcinoma (SCC; CCK168 cells) and mammary carcinoma (EMT6 cells) (Figure 1A), two models in which systemic blockade of TGF-β has been shown to enhance responses to immunotherapy (Dodagatta-Marri et al., 2019; Mariathasan et al., 2018). We injected CCK168 (chemically-induced carcinoma Kras-driven 168) cells subcutaneously into the flanks of syngeneic mice or EMT6 cells directly into the fourth mammary fat pad and allowed tumors to grow to 65–100 mm^3 before beginning antibody therapy. Mice were then injected with ADWA-11 or an isotype-matched control antibody on days 0 and 7 and anti-PD-1 or its isotype-matched control antibody on days 0, 4, and 8. Tumor volume was measured every other day, and mice were euthanized when tumors reached a size of 2,000 mm^3 or more. CCK168 tumors had minimal responses to anti-PD-1, but most mice treated with ADWA-11 monotherapy showed tumor regression, with 4 of 10 mice showing complete tumor regression (Figures 1B and 1C). Combination therapy with ADWA-11 and anti-PD-1 induced complete regression in 9 of 10 tumors, with a significant increase in long-term survival. We then examined the effects of ADWA-11 on the EMT6 model of mammary carcinoma, which has an immune-excluded tumor microenvironment (Mariathasan et al., 2018) and minimal levels of αvβ8 expression (Figure S1E). Anti-PD-1 alone had no effect in this model; ADWA-11 monotherapy had a modest effect, with two mice showing complete regression; and combination therapy substantially and significantly inhibited tumor growth and increased survival (Figures 1D and 1E). 8 of 20 mice demonstrated complete regression of the EMT6 tumor after combined treatment with ADWA-11 and anti-PD-1. The surviving mice treated with ADWA-11 monotherapy (n = 2) or combination therapy (n = 8) were re-challenged with the same number of tumor cells 50 days after initial therapy. No tumors formed in any of these mice, suggesting that successful treatment with ADWA-11 or ADWA-11 and anti-PD-1 can lead to long-term anti-tumor immunity.

To take advantage of genetic tools to evaluate the functional relevance of αvβ8 expression in specific cell types, we also examined the effects of ADWA-11, with or without anti-PD-1, in a C57BL/6 syngeneic model, Transgenic Prostate Cancer 2 (TRAMPC2). TRAMPC2 is a prostatic adenocarcinoma developed from transgenic mice expressing the SV40 large T antigen specifically in prostatic epithelium (Foster et al., 1997). Mice harboring subcutaneous syngeneic TRAMPC2 tumors showed minimal response to anti-PD-1 monotherapy, but tumor growth was reduced markedly by treatment with ADWA-11, with no additional effect of inhibition of PD-1 (Figures 1F and 1G).)

ADWA-11 increases expression of cytotoxic granzyme B in CD8+ T cells and of interferon-γ in CD4+ and CD8+ T cells

We next characterized the effects of ADWA-11 (with or without anti-PD-1) on the nature of the immune infiltrate (Thomas and Massagué, 2005; Wu et al., 2014) in the CCK168 tumor model. Although treatment with anti-PD-1 in this model had no effect on the total number of intratumoral CD8+ T cells, treatment with ADWA-11 significantly increased CD8+ T cell accumulation (Figure 2A). ADWA-11 also significantly increased the percentage of CD8+ T cells that expressed granzyme B and elevated expression of interferon-γ (IFNγ) in CD4+ and CD8+ T cells (Figure 2A), whereas treatment with anti-PD-1 had no effect on these endpoints. We were unable to identify significant production of interleukin-17 (IL-17) in any T cell subsets (data not shown). We also performed immunophenotyping of tumors from untreated mice and mice treated with ADWA-11 of the EMT6 (Figure 2B) and TRAMPC2 (Figure 2C) models. In each of these tumors, ADWA-11 increased CD8+ T cell accumulation, granzyme B expression in CD8+ T cells, and IFNγ expression in tumor CD4+ and CD8+ cells. To confirm whether ADWA-11 increased the total number of CD8 cells in tumors, we stained CD8+ T cells in EMT6 tumors from mice treated with anti-PD-1 or ADWA-11 monotherapy or combination therapy. We found significant increases in CD8+ cells in ADWA-11- but not anti-PD-1-treated tumors (Figure S3A). Regulatory T (Treg) cells are well-known suppressors of anti-tumor immunity, and their numbers could have been reduced by inhibition of TGF-β activation or by antibody-dependent cell-mediated cytotoxicity of αvβ8-expressing Treg cells. We therefore used flow cytometry to determine whether ADWA-11 treatment reduced the fraction of FoxP3+ Treg cells. In each model, ADWA-11 treated animals had more Foxp3+/CD4+ cells, perhaps reflecting a compensatory response to tumor killing and inflammation (Figure S2B). We did not see consistent effects of ADWA-11 on the numbers of CD4+ T cells, macrophages, or dendritic cells. These results suggest that ADWA-11 inhibits *in vivo* tumor growth and enhances the effects of anti-PD-1 by promoting CD8+ T cell accumulation, granzyme B expression in CD8+ T cells, and IFNγ expression in CD4+ and CD8+ T cells.

The beneficial effects of combined ADWA-11 and anti-PD-1 were abrogated by anti-CD8a-mediated T cell depletion

Because the most dramatic effects of ADWA-11 we observed were on CD8+ T cells, we sought to determine whether effects on these cells were responsible for the protective effects of ADWA-11. For this purpose, we treated CCK168 tumor-bearing mice with drugs following removal of CD8+ T cells using a CD8a-depleting antibody. One caveat to this approach is that CD8a is also expressed on a subset of dendritic cells. Immunostaining showed effective CD8+ T cell depletion (Figure S3B), which completely abrogated the beneficial effects of combination therapy with ADWA-11 and anti-PD-1 (Figures 2D and S3C).

Effectorless ADWA-11 inhibits tumor growth, improves survival, and induces persistent anti-tumor immunity in CT26 colon cancer and CCK168 SCC

Because our initial studies were under-taken with native murine ADWA-11, which could have liabilities for clinical development because of activation of Fc receptors, we next

determined whether a version of ADWA-11 engineered to inhibit Fc receptor binding would also have *in vivo* efficacy. We generated a recombinant, effectorless version of ADWA-11 (ADWA-11_4mut) with 4 mutations in the immunoglobulin G1 (IgG1) Fc domain that inhibits binding to all relevant Fc receptors (Figure S1D). This effectorless antibody showed similar potency as wild-type ADWA-11 in inhibition of TGF-β activation by αvβ8 in a co-culture bioassay (Figure S1A) and in adhesion of αvβ8-expressing cells to the TGF-β latency-associated peptide (Figure S1B). We used this antibody in combination with radiotherapy in the CT26 colon carcinoma model. CT26 was tested because it completely lacks detectable αvβ8 expression (Figure S1E) and because radiation therapy has been demonstrated to promote robust tumor growth inhibition when combined with TGF-β receptor inhibitors (Young et al., 2016). Addition of ADWA-11_4mut or anti-PD-1 significantly increased survival of mice when combined with radiotherapy (RT) in this model, with ADWA-11 + RT leading to complete regression in 5 of 9 mice (Figures 3A and 3B). Interestingly, addition of anti-PD-1 to ADWA-11 added little benefit in this model, providing further evidence that inhibition of αvβ8 can be effective even in the absence of additional checkpoint inhibitors. The surviving mice that received monotherapy or combination therapy were re-challenged with the same tumor cells more than 50 days after initial therapy in the CCK168 and CT26 models. Minimal tumor growth was observed, less than 100 mm^3, and the tumors that did grow out subsequently regressed despite no further treatment, suggesting that successful treatment with ADWA-11_4mut can also lead to long-term anti-tumor immunity, as described previously for other immunomodulators, including TGF-β blockade (Figure 3C; Ascierto et al., 2017; Batlle and Massagué, 2019; Dodagatta-Marri et al., 2019). In preparation for clinical trials, a humanized version of ADWA-11_4mut was evaluated for toxicity in mice and cynomolgus monkeys for 1 month at doses more than 10 times those used here, and no gross or microscopic evidence of adverse or severe toxicity was observed (data not shown).

ADWA-11_4mut enhances the effects of anti-CTLA-4 and 4-1BB in the EMT6 mammary carcinoma model

We next sought to determine whether effectorless ADWA-11 might broadly enhance the beneficial effects of additional immunomodulatory therapies. For this purpose, we examined anti-CTLA-4, which has been shown recently to work in part by a different molecular mechanism than anti-PD-1 (Wei et al., 2017), and an agonist antibody against 4-1BB, an activator of the inducible costimulatory receptor CD137. We used the EMT6 model, in which ADWA-11 monotherapy was only minimally effective. In this model, anti-CTLA4 and anti-4-1BB caused modest reductions in the time to reach the terminal endpoint of tumor growth, but only one mouse treated with anti-4-1BB alone and none treated with anti-CTLA4 survived (Figures 4A and 4B). In contrast, approximately 60% of mice treated with ADWA-11 in combination with anti-CTLA4 or 4-1BB were long-term survivors. As we found for the CCK168 and CT26 complete responders, re-challenge of all long-term survivors in the combined therapy groups showed minimal tumor growth followed by rapid tumor elimination, suggestive of long-term anti-tumor immunity (Figure 4C).

ADWA-11 treatment inhibits TGF-β/Smad3 signaling in tumors and increases expression of genes normally repressed by TGF-β in CD8+ T cells

As noted above, all of the previously identified effects of tissue-specific knockout of *Itgb8* could be explained by loss of TGF-β signaling activity. To determine the contribution of αvβ8 to overall TGF-β activity in tumors, we measured the effects of ADWA-11 on phosphorylation of the early TGF-β signaling effector SMAD3 by western blotting of whole-tumor lysates. ADWA-11 significantly inhibited pSMAD3 in CCK168, EMT6, and TRAMPC2 tumors, suggesting that αvβ8 is a major contributor to TGF-β activation in each of these tumor models (Figure 5A). Because our immunophenotyping and CD8+ depletion results suggested that CD8+ T cells are the functionally important target of ADWA-11 treatment, we sought to determine whether ADWA-11 might act by inhibiting TGF-β presentation to CD8+ T cells with consequent inhibition of TGF-β signaling in these cells. We therefore sought to investigate downregulation of more stable markers of TGF-β signaling. Previous work by Thomas and Massagué (2005) identified a group of genes that were repressed significantly *in vitro* by activated CD8+ T cells treated with active TGF-β1. We used qRT-PCR to interrogate expression of a panel of these genes (granzyme B, IFNγ, granzyme A, and Fas ligand) that we chose because each of them could play a role in enhanced CD8+ T cell-mediated tumor killing. Expression of all but one of these genes was upregulated significantly in CD8+ T cells sorted from CCK168 and EMT6 tumors (Figures 5B and 5C), and all four genes were upregulated significantly in CD8+ T cells from ADWA-11-treated TRAMPC2 tumors (Figure 5D), suggesting that ADWA-11-mediated tumor suppression might, at least in part, be a consequence of inhibition of TGF-β presentation to CD8+ T cells. However, because we were unable to obtain enough protein from CD8 T cells purified from tumors to perform western blotting for pSMAD3, we cannot be certain that the TGF-β activated by αvβ8 acts directly on CD8 T cells.

Characterization of integrin αvβ8 expression on immune cells in the tumor microenvironment

Flow cytometry of *in vitro* cultures of each of the four tumor types studied showed a broad range of expression of αvβ8, with high expression in CCK168 and TRAMPC2 cells, minimal expression in EMT6 cells, and undetectable expression in CT26 cells (Figure S1D). Unlike the cases for cells in culture, none of the antibodies we evaluated against αvβ8 were able to reliably detect this integrin on cells disaggregated from *in vivo* tumors. We therefore used flow cytometry to sort a variety of cell types (Figure S4A) from three tumor types representing a range of αvβ8 expression on tumor cells (CCK168, EMT6, and TRAMPC2) and evaluated *Itgb8* mRNA expression by qRT-PCR (Figure 6A). *Itgb8* expression was consistently seen at the highest levels on CD4+CD25+ T cells. These were the major T cell population expressing the Treg cell marker *FoxP3*. Even in CCK168 and TRAMPC2 tumors, where the tumor cells *in vitro* expressed easily detected surface expression of αvβ8, the level of *Itgb8* RNA expression was minimal in tumor cells harvested from *in vivo* tumors. *Itgb8* expression in these tumors was more than 10 times higher in tumor-derived CD4+CD25+ T cells than in tumor cells (Figure 6A). Importantly, *Itgb8* RNA expression was 3-to 5-fold higher in CD4+CD25+ T cells of the tumor compared with those isolated from spleen or tumor-draining lymph nodes (Figure S4C).

ADWA-11 blocks the suppressive effects of CD25+CD4+ T cells on CD8 T cell-mediated tumor cell killing *in vitro*

We next used a simplified *in vitro* co-culture system to directly examine whether ADWA-11 treatment enhanced the ability of tumor CD8+ T cells to kill tumor cells. We co-cultured CD8+ T cells sorted from tumors with relevant tumor cells and used AnnexinV staining to quantify tumor cell death. CD8+ T cells from EMT6 or TRAMPC2 tumors obtained from ADWA-11-treated mice were significantly more effective in killing tumor cells than CD8+ T cells obtained from control mice (Figure S5A). We then performed similar assays using CD8+ T cells from TRAMPC tumors grown in untreated mice with or without addition of ADWA-11 and/or CD25+/CD4+ T cells, a population enriched for Treg cells. The cytotoxic effect of CD8 T cells was inhibited by addition of CD25+/CD4+ cells, and this suppressive effect was inhibited significantly when CD25+/CD4+ cells were pretreated with ADWA-11. ADWA-11 in this system had no effect on baseline tumor death or on tumor cell killing induced by CD8 T cells alone (Figure S5B). These results suggest that αvβ8 expressed on CD25+/CD4+ T cells can act directly on CD8+ T cells to suppress tumor cell killing.

Specific deletion of Itgb8 from T cells delays *in vivo* tumor outgrowth and is redundant to effects of ADWA-11 on tumor growth inhibition

Because we found high expression of αvβ8 in CD4+CD25+ T cells, we next sought to determine whether genetic deletion of *Itgb8* in T cells could recapitulate the suppressive effects of ADWA-11 on tumor growth. We generated CD4-Cre;*Itgb8*-f/f mice in which *Itgb8* is deleted in all T cells. TRAMPC2 tumor cells were injected into CD4-Cre;*Itgb8*-f/f and *Itgb8*-f/f littermates, and mice in both groups were left untreated or treated with ADWA-11. Tumor growth was suppressed significantly (Figures 6B and S6A), and survival was enhanced in CD4-Cre;*Itgb8*-f/f mice compared with *Itgb8*-f/f littermates. As we found previously for control mice, ADWA-11 significantly inhibited growth and enhanced survival in Cre-negative *Itgb8*-f/f mice. Adding ADWA-11 showed no additional benefit in CD4-Cre;*Itgb8*-f/f mice. We next characterized the effects of immune infiltration in mice with genetic deletion of *Itgb8* in T cells. As we found in mice treated with ADWA-11, deletion of *Itgb8* in T cells significantly increased CD8+ T cell accumulation in TRAMPC2 tumors and significantly increased expression of granzyme B and IFNγ in CD8+ T cells. There was also a trend toward elevation of IFNγ and Foxp3 expression in CD4+ T cells that did not reach statistical significance (Figure S6C). We also found that expression of granzyme A and B, IFNγ, and Fasl was increased in CD8+ T cells from tumors of mice lacking *Itgb8* (Figure S6D). CD8+ T cells from CD4-Cre;*Itgb8*-f/f mice also showed greater tumor cell killing ability *in vitro* than T cells from *Itgb8*-f/f littermates (Figure S6E). These data suggest that αvβ8-mediated suppression of tumor immunity in this model is largely due to αvβ8 expression by CD4+/C25+ T cells. Because we and others have previously described functionally important effects of deletion of *Itgb8* from dendritic cells, we performed similar experiments in mice in which *Itgb8* was deleted from dendritic cells (CD11c-Cre;*Itgb8*-f/f) but found no effect of this deletion on tumor growth or survival (Figures 6C and S6B).

DISCUSSION

In this study, we show that ADWA-11, a blocking monoclonal antibody specific for the αvβ8 integrin, can inhibit tumor growth and enhance CD8+ T cell expression of a suite of genes involved in tumor killing in multiple syngeneic tumor models. ADWA-11 also dramatically enhances responses to multiple immunomodulators (anti-PD-1, anti-CTLA-4, and 4-1BB) and to RT. Depletion of CD8+ T cells abrogates the beneficial effects of ADWA-11 and anti-PD-1 treatment, suggesting that enhanced tumor cell killing by CD8+ T cells is critical for the anti-tumor effects of ADWA-11. In every model we examined, the highest level of *Itgb8* mRNA was found in CD4+CD25+ T cells, a population enriched in Treg cells. Furthermore, knockout of *Itgb8* specifically in T cells mimicked the effects of ADWA-11, suggesting that αvβ8 expressed on T cells plays an important role in suppression of anti-tumor immunity. Because the major T cell subset we found to consistently express high levels of *Itgb8* in tumors was CD25+CD4+ cells, we suspect that Tregs might be the cells responsible for this effect.

All previously described effects of loss of αvβ8 *in vivo* can be explained by contextual loss of activation of TGF-β, so we suspect that inhibition of TGF-β activation is responsible for these effects (Melton et al., 2010; Mu et al., 2002; Travis et al., 2007; Worthington et al., 2015). This hypothesis is supported by our observation that ADWA-11 significantly inhibited overall tumor TGF-β signaling in all of the models we studied and by our finding that a suite of genes involved in antigen-triggered cytotoxicity, including granzyme A and B, IFNγ, and Fasl, which have all been shown previously to be inhibited by TGF-β in CD8+ T cells (Thomas and Massagué, 2005), were coordinately increased in CD8+ T cells purified from tumors in mice treated with ADWA-11. CD8+ T cells from ADWA-11 treated mice exhibited enhanced tumor killing ability *in vitro*. Tumor killing by CD8+ T cells was suppressed by co-culture with CD25+CD4+ T cells, and this effect was inhibited significantly by incubation of these cells with ADWA-11. These results suggest that TGF-β activated by αvβ8 expressed on CD25+CD4+ T cells inhibits tumor immunity at least in part by directly suppressing the cytotoxic program in CD8+ T cells. Short-term therapy with ADWA-11 and immunomodulators or RT led to long-term tumor suppression and resistance to subsequent re-challenge, strongly supporting induction of long-term anti-tumor immunity.

It is important to point out that the antibody we used to deplete CD8 T cells targets CD8a, which is also expressed on a subset of dendritic cells. We therefore cannot exclude the possibility that the complete reversal of the protective effects of ADWA-11 we observed after antibody-mediated depletion was in part due to depletion of this subset of dendritic cells. However, our *in vitro* findings that CD8 T cells from mice treated with ADWA-11 had increased granzyme B expression and increased capacity to kill tumor cells is at least consistent with the hypothesis that CD8 T cells are critical effectors of the beneficial effects of ADWA-11.

One previous study described inhibition of tumor growth by treatment with an antibody against αvβ8, but the authors of that paper suggested that αvβ8 expression on tumor cells was critical for this effect (Takasaka et al., 2018). Because they did not detect αvβ8 expression by T cells using flow cytometry, they concluded that this integrin was only

expressed on tumor cells. However, in this study, and in studies published previously showing functional effects of αvβ8 on Treg cells (Stockis et al., 2017; Worthington et al., 2015), none of the available αvβ8 anti-bodies could detect αvβ8 by flow cytometry on Treg cells. The basis for this limitation of antibodies for flow cytometry is not known, but we speculate that the epitopes recognized by these antibodies are not accessible on Treg cells, perhaps because they are masked by other proteins (for example GARP) present in complex with αvβ8. In the current study, we employed a range of tumor models, including some in which tumor cells expressed αvβ8 and others in which there was little or no detectible expression of *Itgb8* mRNA or αvβ8 protein, and found effects of αvβ8 blockade that did not appear to be strongly correlated with the level of αvβ8 expression on tumor cells. Our observations that deletion of *Itgb8* from T cells is as effective as systemic inhibition by ADWA-11 and that administration of ADWA-11 to mice lacking *Itgb8* on T cells does not further inhibit tumor growth strongly suggest that the effectiveness of the αvβ8-blocking antibody is not simply due to blocking αvβ8 on tumor cells. Our results should not be interpreted as demonstrating that αvβ8 on tumor cells does not contribute, under some circumstances, to suppression of anti-tumor immunity. Our finding in the current paper is that inhibition of αvβ8 on T cells also plays a major role.

A previous study demonstrated combined effects of anti-PDL-1 and systemic blockade of TGF-β in the EMT6 model and, like us, also showed that CD8 depletion abrogated these effects and that the effect on tumor growth was associated with accumulation of granzyme B-expressing CD8+ T cells within the tumors. However, in that study, inhibition of TGF-β alone had no effect on tumor regression or accumulation of granzyme B-expressing CD8+ cells, whereas in the current study, we saw clear effects of monotherapy with our αvβ8-blocking antibody. We think the difference may be due to the large amount of TGF-β ligand present *in vivo* compared with the relatively low expression of αvβ8 on T cells. αvβ8 integrin is not widely expressed in adult mammals, and when it is expressed, it is present at only several thousand receptors per cell. In contrast, TGF-β isoforms are stored diffusely as latent complexes bound to the extracellular matrix in many tissues, making complete inhibition of these ligands difficult to achieve. However, because we did not directly compare TGF-β-blocking antibodies with ADWA-11 in the EMT6 model, we cannot make definitive statements about relative efficacy. Of course, we cannot absolutely exclude the possibility that αvβ8 has effects on anti-tumor immunity that are independent of inhibition of TGF-β activation, but so far, no such effects have been demonstrated convincingly.

In this study, we were able to show that treatment with ADWA-11 decreased global TGF-β signaling, as assessed by western blotting for pSMAD3 in whole-tumor lysates, consistent with previous evidence showing that TGF-β activation is the principal role of αvβ8 *in vivo*. However, because of the large amount of input protein required to assess TGF-β signaling by western blotting, we were not able to determine whether the activated TGF-β acted directly on CD8 T cells.

In this report, we show that αvβ8 integrin is expressed on CD25+CD4+ T cells in multiple syngeneic tumor models and is a potent modulator of the anti-tumor immune response. Although efficacy was seen for monotherapy targeting this integrin in most of the tumor models we studied, efficacy can be improved substantially by combining inhibition of αvβ8

with the checkpoint inhibitors anti-PD-1 or anti-CTLA4 or the immune activator 4-1BB or by combining αvβ8 monotherapy with RT. Intriguingly, we found that αvβ8 expression was much higher on intratumoral CD4+CD25+ T cells than in those isolated from draining lymph nodes and the spleen, a feature that might benefit immune-mediated tumor rejection by this drug while minimizing harm to normal tissues that might arise from reduced peripheral tolerance. These results identify αvβ8 as a promising target for tumor immunotherapy.

STAR★METHODS

RESOURCE AVAILABILITY

Lead contact—Further information and requests for resources and reagents should be directed to and will be fulfilled by the lead contact, Dean Sheppard (dean.sheppard@ucsf.edu).

Materials availability—The murine monoclonal antibody, ADWA11, described in this manuscript is available is available from Dean Sheppard. There were no other unique reagents generated.

Data code and availability—The published article includes all datasets generated or analyzed during this study.

EXPERIMENTAL MODEL AND SUBJECT DETAILS

Animal or mouse models—Mice were bred and maintained according to approved protocols by the University of California, San Francisco, or Pfizer Inc., Institutional Animal Care and Use Committee. Wild-type FVB mice were purchased from Jackson Laboratories (The Jackson Laboratories, stock #001800). Wild-type BALB/c mice were purchased from Charles River Laboratories (Charles River Laboratories, strain code 028). Wild-type C57/B6 mice were purchased from Jackson Laboratories (The Jackson Laboratories, stock #001800). Mice with conditional deletion of itgb8 from T cells were bred by crossing CD4-cre mice (Tg(Cd4-cre)1Cwi/BfluJ, stock number 017336) obtained from Jackson Laboratories with itgb8 f/f mice obtained from Louis Reichardt at UCSF. For studies of syngeneic breast cancer (EMT-6) only female mice were used and for prostate cancer (TRAMPC2) only male mice were used. Otherwise equal numbers of male and female mice were used and cage mates were randomly assigned to experimental groups. No effects of sex were detected.

Cell lines—All cell lines and primary cells were grown at 37°C in 5% CO2 and maintained as sub-confluent cultures. CCK168 cells, derived from a male murine, chemically induced squamous cell carcinoma, were generated and obtained from Allan Balmain (UCSF). EMT6 cells (derived from a female triple negative murine breast cancer (ATCC CRL2731), TRAMPC2 cells (derived from a male murine prostatic cancer (ATCC CRL2731) and CT26 cells (derived from a male murine colon cancer, ATCC CRL-2638) were all obtained from and validated by ATCC. C8-S cells a murine male astrocyte cells line and SNB19 cells, a human male glioblastoma cell line (ATCC CRL2219) and C8-D1A (a murine female astrocyte cell line ATCC CRL2541) were also obtained from and validated by ATCC.

SW480 cells, a human male colon carcinoma cell line was a gift from Michael Agrez, U. Newcastle.

METHOD DETAILS

Tumor models—CCK168 cells, a chemically induced squamous cell carcinoma cell line derived from FVB mice[6], were injected subcutaneously in the right flank region in syngeneic wild-type FVB mice (1.5×10^4 cells/mouse). Tumors were allowed to grow over 14 days. Mice selected for the experiment had tumor size at least 0.5 cm in diameter and were randomized to different antibody treatment groups using a random number generator (https://www.random.org). The study team was blinded to the treatment groups of 10 mice per group. Mice were weighed daily, and tumor size was measured every other day for the duration of the study using a traceable digital caliper (Fisher Scientific, model #14-648-17). Mice were euthanized when tumor size exceeded 2000 mm^3 or developed a large ulceration at the tumor site. Appropriate antibody for each group and isotype control antibodies were injected on days 0, 4, and 8 of the experiment for anti-PD-1 and day 0 and 7 for ADWA-11. Doses of intraperitoneal antibodies injected were ADWA-11 (10 mg/kg), Anti-PD-1 (10 mg/kg), control antibody ADWA-21 (for ADWA-11, 10 mg/kg), and control 2A3 (for PD-1, 10 mg/kg). Control ADWA-21 binds only human integrin-β8, but not mouse integrin-β8. For CD-8 depletion studies, intraperitoneal anti-CD-8 (Bio X Cell® BE0004–1 Clone 53–6.72) or control antibody was injected at a dose of 10 mg/kg on days 0, 4, and 8. Combined ADWA-11 (10 mg/kg) and anti-PD-1 (10 mg/kg) were injected on days 1, 5, and 9 in the CD8 depletion studies.

EMT6 (ATCC®, CRL2755) cells, a mouse epithelial mammary carcinoma cell line, were injected into the fourth mammary fat pad (5×10^4 cells/mouse) of BALB/c mice, and mice were followed daily until the tumors reached 0.5 cm for inclusion in the study (Zhang et al., 2016). Subsequent treatment regimens and measurements were performed as above.

TRAMPC2 (ATCC®, CRL2731) cells, a mouse epithelial prostate adenocarcinoma cells were injected subcutaneously in the right flank region in syngeneic wild-type C57/B6 mice (1×10^6 cells/mouse with matrigel). Tumors take about four weeks to reach 100$mm^{\#}$ for the treatment that described as above.

CT26 mouse colon carcinoma cells (ATCC® CRL-2638, 2.5×10^5 cells/mouse) were injected into the subcutaneous flank of female BALB/c mice (Charles River Labs). Tumors were allowed to grow to 50–100 mm^3 in size for inclusion in the study. For these studies, ADWA-11_4mut or isotype control 2B8_mIgG_4mut were injected on days 0, 4, 8, 12, anti-PD-1 (RMP1–14, BioXcell) or isotype control 2A3_rat IgG (BioXcell) were injected on days 0, 4, 8 through an intravenous route. All antibodies were dosed at 10mg/kg. All mice on Day 5, except the no treatment control group, were exposed to tumor targeted 5 Gy dose of radiation. Tumor growth was measured twice per week with digital calipers and reported as volume (length × width × width × 0.5). For the re-challenge experiment, on day 51 (post first antibody treatment) mice with a complete response and naive mice were implanted on the contralateral flank with 2.5×10^5 CT26 cells in PBS and tumor growth was monitored as described above.

ADWA-11_4mut was also tested in the EMT-6 tumor model. 1×10^6 EMT6 cells (ATCC®, CRL2755) were injected into the fourth mammary fad pad of female BALB/c mice (Charles River Labs). Tumors were allowed to grow up to 50–100 mm^3 in size. Mice were randomized into antibody treatment groups and operators were blinded to treatment groups. ADWA-11_4mut 10mg/kg or control 2B8_mIgG4mut 10mg/kg, anti-CTLA4 (9D9 BioXcell) or isotype control E.tenella-mIgG2b 10mg/kg were injected on days 0, 4 and 8, and 4-1BB (MAB9371, R&D systems) 1mg/kg was injected on days 0 and 4 through an intravenous route. Tumor growth was measured twice per week with digital calipers and reported as volume (length × width × width × 0.5). For the re-challenge experiment, on day 51 (post first antibody treatment) mice with a complete response and naive mice were implanted in the contralateral fat pad with 1×10^6 EMT-6 cells and tumor growth was monitored as described above.

Generation of avβ8 blocking antibody ADWA-11—Integrin β8 knockout mice, crossed into the outbred CD1 background to permit post-natal survival were immunized with recombinant αvβ8 integrin (R&D Systems, 4135-AV-050) 50 μg per mouse every two weeks. Sera from immunized mice were screened by solid phase immunoassays and used to identify mice for hybridoma generation. Antibodies from the hybridomas were labeled with APC fluorophore and further characterized by flow cytometry using SW480 cells, which normally do not express any αv integrins except αvβ5, were transfected to express integrin αvβ8 or αvβ3 or αvβ6 as negative controls. We performed flow cytometry on each cell line using labeled ADWA-11 or antibodies to αvβ5 (Alula) or αvβ3 (Axum-2) or αvβ6 (10D5) (Huang et al., 1998; Su et al., 2012; Su et al., 2007). Cell adhesion assays were performed with SNB19 cells (ATCC®, CRL2219 human glioblastoma cell line) that express integrin αvβ8 on dishes coated with TGFβ1 latency associated peptide 1 μg/ml (Kueng et al., 1989) in the presence of ADWA-11 and ADWA-11_4mut in concentrations from 0.067 to 66.67 pM. Adherent cells were stained with crystal violet and adhesion expressed as absorbance at 595 nm. Blockade of TGFβ activity was determined by TMLC luciferase assay (mink lung epithelial cells expressing a TGFβ sensitive portion of PAI-1 promoter driving firefly luciferase expression) (Abe et al., 1994). TMLC cell (15,000/well) was co-cultured with SNB229 (ATCC®, CRL2611) (50,000/well) that express integrin αvβ8 in the presence of ADWA-11 and ADWA-11_4mut ranging from 0.067 to 66.67 pM. TGFβ activity is reported as relative luciferase units based on PAI-1 luciferase reporter activity after 16hrs.

Biacore studies of binding of 4 mut Fc domain to murine FcRs—Two sets of mouse antibody variants, mu3D6 (mu3D6-IgG2a wt, mu3D6-IgG1 wt and mu3D6-IgG1 4 m) and mu12A11 (mu12A11-IgG2a wt, mu12A11-IgG1 wt and mu12A11-IgG1 4 m) were used to compare their Fcγ receptor binding. The *in vitro* binding of these antibodies to the recombinant extracellular domains of three mouse Fcγ receptors, muFcγRI (an activating receptor), muFc-γRII (an inhibitory receptor) and muFcγRIII (an activating receptor), were assessed using a surface plasmon resonance (SPR) based assay.

Biacore 3000 and a CM5 chip coated with Penta-His antibody (QIAGEN, Cat #34660) were used to test the binding of antibodies to the extracellular domains of recombinant mouse Fcγ receptors. The monoclonal extracellular domains of muFcγRI, muFcγRII, and muFcγRIII,

all with a His tag at the C-termini, were purchased from the R&D Systems (Cat# 2074-Fc, 1460-CD, 1960-Fc). One receptor was captured in one flow cell of a sensor chip by the pre-immobilized anti-His antibody (Penta-His). An antibody solution was then injected to enable the measurements of the association and the dissociation rates of binding to the captured receptor. Following the measurements, all captured receptor, with and without a bound antibody, were removed from the flow cell by the injection of a pH 2.5 buffer. The flow cell was then ready for the next cycle of receptor-capturing and antibody-binding. Each experiment was carried out in duplicate. To enable quantitative comparisons, the same experimental conditions (i.e., same amount of captured receptor, same concentration, time and flow rate for the antibody injections) were applied to all receptors. The sensorgrams were "double corrected" for the reference flow cell signals and the buffer injection responses.

Generation of effectorless ADWA-11 antibody (ADWA-11_4mut)—To construct an anti-αvβ8 antibody with reduced Fc receptor binding and effector function the variable regions from ADWA11 were subcloned into a mIgG1 Fc backbone that contained E233P, E318A, K320A, and R322A mutations, as outlined in https://patents.google.com/patent/US20090155256. ADWA-11_4mut binding to mouse αvβ8 was assessed using C8-D1A mouse astrocyte cells (ATCC, CRL2541) and blockade of TGFβ activation was determined using C8-S cells in a co-culture TMLC luciferase assay, described above.

Flow cytometry—Subcutaneous tumors were isolated from the mice using scissors and blunt dissection. The tumors were placed in a Petri dish with digestion cocktail of Collagenase XI (Sigma C9407) 2 mg/mL, Hyaluronidase (Sigma H3506) 0.5 mg/ML, and DNase (Sigma DN25) 0.1 mg/mL prepared in C10 media (RPMI 1640, HEPES 1%, Penicillin/Streptomycin 1X, fetal calf serum 10%, sodium pyruvate 1 mM, non-essential amino acids 1X, and beta-mercaptoethanol 0.45%). Tumors were minced using sterile scissors. The resultant slurry of cells was transferred into 50 mL conical tubes (Fisher Scientific #14-432-22) and the Petri dish used to mince the tumor was rinsed with 2 mL C10 media to capture remaining cells. Cells were incubated in a shaker at 255 rpm for 45 minutes at 37°C. After incubation, 15 mL of C10 media was added to the digested tumor cells and gently vortexed for 15 s. The cell slurry was passed through a 100 μm mesh strainer (Falcon® #352360) into a clean 50 mL conical tube. Cells were pelleted by centrifugation for 5 minutes at 200 g at 4°C and reconstituted in PBS. Cell counts were performed using a hemo-cytometer (Fisher Scientific #02-671-6).

Isolated single cell preps were used for cell surface and intracellular staining. After counting, 10×10^6 cells were transferred into each well of a v-shaped 96-well plate for staining. Live dead staining with Ghost Dye Violet 510 (TONBO bioscience#13–0870) at 1:1000 for 20 minutes at 4°C. Fc receptor and non-specific binding was blocked with anti-CD16/30 (eBioscience #14061) for 10 minutes at 4°C. Surface staining was performed for 20 minutes at 4°C. For intracellular staining, cells were incubated in Fix/Perm buffer (eBioscience #88–8824) for 20 minutes at room temperature followed by intracellular cytokine staining with antibody cocktails for 20 minutes at 4°C. After completion of

staining, cells were transferred into flow cytometry buffer (PBS with 2%FBS, Penicillin/Streptomycin/Glutamate, EDTA 2 mM) for analysis.

Antibodies used for intracellular cytokine staining experiments: CD45 AF700 (Invitrogen#56-0451-80), CD3e BV711 (Biolegend#100241), CD25 BV605 (BioLegend#102036), CD4 APC-Cy7(Invitrogen#47-0042-82), CD8a PE Cy7 (eBioscience#25-0081-81), NKG2A/C/E APC (Biolegend 564383), Granzyme-B PE (eBioscience#12-8898-82), FoxP3 PB-e450 (eBioscience#48-5773-82), IFNg BV650 (BioLegend#505831)

For cell stimulation, cells were stimulated prior to cell surface and intracellular staining. Approximately 3×10^6 cells in 200 μL of C10 media per well were incubated in round-bottom 96-well plates overnight in a tissue culture incubator in 5% CO2 at 37°C. Stimulation cocktail (Inomycin, PMA, Brefeldin-A, and Monensin 500x stimulation cocktail Tonbo #TNB4975-UL100) was added to cells which were incubated in tissue culture incubator in 5% CO2 at 37°C. for 4 hours. Cells were transferred to v-bottom wells for staining as outlined above.

Antibodies used for cell sorting experiments (Lymphocyte panel): CD45 AF700 (Invitrogen 56-0451-80), B220 PerCP Cy5.5 (eBio-sciences 45-0452-80), CD8a PE-Cy7(eBiosciences 12-0081-81), CD4 APC-Cy7(Invitrogen 47-0042-82), NKG2A/C/E APC (Biolegend 564383), CD3e BV711 (Biolegend 100241), CD25 BV605 (BioLegend#102036)

Antibodies used for cell sorting experiments (Myeloid panel): CD45 AF700 (Invitrogen 56-0451-80), CD64 FITC (BioLgend#139307), Cd11b PE-Cy7 (BioLegend#101215), Thy1.2 BV421 (BioLegend#105341), Thy1.1 BV421 (BioLegend#202529), (Cd11c BV605 (BioLegend#117334), MHCII PE/Dizzle(BioLegend#107648).

Flow cytometry was performed using a Attune NxT Flow Cytometer (ThermoFisher). Cell sorting was performed using a BD FACSAria3 (BD Biosciences) and analyzed using FlowJo (Tree Star Inc.).

Tumor apoptosis assay—CD8+ and CD25+CD4+ T cells were FACS sorted (gating strategy has been described above) from tumor and collected in RPMI1640 culture medium containing 10%FBS, 1X Glutamax. Sorted cells were seeded as 3000 cells/well into 96-well plate with relevant tumor cells that had been pre-seeded (10,000/well) 6–8hrs ahead. After 48hrs co-culture, cells were trypsinized and transferred to 96-well V-shape plate for Annexin V (BioLegend#640909) staining. Flow cytometry was performed to quantify the Annexin V + population.

Quantitative PCR analysis—Total RNA was isolated from sorted tumoral cells using Trizol Reagent (Life Technologies) according to the manufacture's instruction. RNA was reverse transcribed by SuperScript IN VILO master mix(Invitrogen) with DNase treatment. Power SYBR Green master mix(Life Technologies) was used for quantification of cDNA on QuantStudio 5 Real Time PCR system (Thermo-Fisher). Primers used were listed in Table S1.

Western blotting—Tumors were harvested and homogenized in 500ul RIPA lysis buffer (50 mM Tris-HCl, pH 8, 150 mM NaCl, 1% NP-40, 0.1% SDS, 0.5% sodium deoxycholate) containing protease and phosphatase inhibitors (ThermoFisher Scientific). Tumor lysate protein concentration was measured using Pierce BCA Protein Assay (ThermoFisher Scientific). Tumor lysate then boiled at 95 C on a heat block in Laemmli sample buffer (4% SDS, 10% 2-mercaptoethanol, 20% glycerol, 0.004% bromophenol blue, 0.125 M SDS, pH 6.8), separated by electrophoresis on a 10% polyacrylamide gel, and transferred to a polyvinylidene difluoride membrane (Millipore Sigma). The primary antibodies and dilutions were as follows: Rabbit anti-pSMAD3 Ab (Abcam ab52903 1:1000), tSMAD3(Abcam ab40854 1:1000) and anti-β-actin Ab (Sigma, a5441, 1:5000). Secondary antibodies were horseradish peroxidase (HRP) conjugated goat anti rabbit (Cell Signaling Technology, 1:3000) or goat anti mouse (Cell Signaling Technology, 1:5000). Chemiluminescent HRP substrate (PerkinElmer) was used for membrane development. Immunoreactive bands were visualized with a Mini-Med 90 X-Ray Film Processor (AFP Imaging). Band densitometry was performed using ImageJ software.

Immunostaining—Tumors were harvested and fixed in 4% paraformaldehyde at 4°C for 3 hours. The fixed tumors were immersed in 30% sucrose solution at 4°C overnight and embedded in O.C.T. compound (Tissue Tek® #4583). Frozen sections were stained by previously described protocols (Henderson et al., 2013; Rock et al., 2011). Antibodies used for immunostaining: FITC-conjugated or Alexa Fluor 594-conjugated anti-mouse CD8 antibody (BioLegend, clone 53–6.7). Confocal microscopy was performed on a Zeiss LSM 780 microscope. Fluorescence intensity were analyzed by using ImageJ software.

QUANTIFICATION AND STATISTICAL ANALYSIS

One-way ANOVA was applied to compare three or more groups and post hoc Tukey-Kramer tests were used to identify specific differences (Figures 2, S5, and S6). Unpaired two tail t test was used to compare two groups to determine significant change (Figures 2, 5, S2, S3, and S6). Values are reported as mean ± standard division (SD). N = number of animals (Figures 1, 2, 3, 4, 5, 6, S2, and S6) or number of biologic samples (Figures S1, S5, and S6). In survival studies, comparison of survival curves was calculated based on Log-rank Mantel-Cox test (Figures 1, 2, 3, 4, and 6). Statistical analysis was performed using GraphPad Prism 5.0, Graphpad Software, San Diego, California, USA.

Supplementary Material

Refer to Web version on PubMed Central for supplementary material.

ACKNOWLEDGMENTS

This work was supported by a grant from the joint UCSF-Pfizer Centers for Translational Innovation (CTI) (to D.S. and R.J.A.), NCI R01CA197198 (to R.J.A.). This work was supported by the National Cancer Institute's Office of Cancer Genomics Cancer Target Discovery and Development (CTD^2) initiative, NCI CTD2 grant U01CA217864 (PI, William Weiss). The work was supported by use of UCSF HDFCCC shared resource facilities, the Laboratory of Cell Analysis, and the Preclinical Therapeutics Core. J.L. was supported by NIH KHL111208A. The results published here are based in whole or in part upon data generated by Cancer Target Discovery and Development (CTD^2) Network (https://ocg.cancer.gov/programs/ctd2/data-portal) established by the National Cancer Institute's Office of Cancer Genomics.

DECLARATION OF INTERESTS

D.S. and R.J.A. were funded by a grant from the joint UCSF-Pfizer CTI. S.Y., A.G., K. Noorbehesht, B.Y., K. Niessen, and J.D.P. were employees of Pfizer. UCSF and Pfizer have filed a joint patent covering the use of a humanized version of ADWA-11 for cancer immunotherapy.

REFERENCES

Abe M, Harpel JG, Metz CN, Nunes I, Loskutoff DJ, and Rifkin DB (1994). An assay for transforming growth factor-beta using cells transfected with a plasminogen activator inhibitor-1 promoter-luciferase construct. Anal. Biochem 216, 276–284. [PubMed: 8179182]

Akhurst RJ, and Hata A (2012). Targeting the TGFβ signalling pathway in disease. Nat. Rev. Drug Dev 11, 790–811.

Ascierto PA, Daniele B, Hammers H, Hirsh V, Kim J, Licitra L, Nanda R, and Pignata S (2017). Perspectives in immunotherapy: meeting report from the “Immunotherapy Bridge”, Napoli, November 30th 2016. J. Transl. Med 15, 205. [PubMed: 29020960]

Batlle E, and Massagué J (2019). Transforming Growth Factor-β Signaling in Immunity and Cancer. Immunity 50, 924–940. [PubMed: 30995507]

Bragado P, Estrada Y, Parikh F, Krause S, Capobianco C, Farina HG, Schewe DM, and Aguirre-Ghiso JA (2013). TGF-β2 dictates disseminated tumour cell fate in target organs through TGF-β-RIII and p38α/β signalling. Nat. Cell Biol 15, 1351–1361. [PubMed: 24161934]

Derynck R, Turley SJ, and Akhurst RJ (2021). TGFβ biology in cancer progression and immunotherapy. Nat. Rev. Clin. Oncol 18, 9–34. [PubMed: 32710082]

Dodagatta-Marri E, Meyer DS, Reeves MQ, Paniagua R, To MD, Bin-newies M, Broz ML, Mori H, Wu D, Adoumie M, et al. (2019). α-PD-1 therapy elevates Treg/Th balance and increases tumor cell pSmad3 that are both targeted by α-TGFβ antibody to promote durable rejection and immunity in squamous cell carcinomas. J. Immunother. Cancer 7, 62. [PubMed: 30832732]

Flavell RA, Sanjabi S, Wrzesinski SH, and Licona-Limón P (2010). The polarization of immune cells in the tumour environment by TGFbeta. Nat. Rev. Immunol 10, 554–567. [PubMed: 20616810]

Foster BA, Gingrich JR, Kwon ED, Madias C, and Greenberg NM (1997). Characterization of prostatic epithelial cell lines derived from transgenic adenocarcinoma of the mouse prostate (TRAMP) model. Cancer Res. 57, 3325–3330. [PubMed: 9269988]

Gorelik L, and Flavell RA (2001). Immune-mediated eradication of tumors through the blockade of transforming growth factor-beta signaling in T cells. Nat. Med 7, 1118–1122. [PubMed: 11590434]

Henderson NC, Arnold TD, Katamura Y, Giacomini MM, Rodriguez JD, McCarty JH, Pellicoro A, Raschperger E, Betsholtz C, Ruminski PG, et al. (2013). Targeting of αv integrin identifies a core molecular pathway that regulates fibrosis in several organs. Nat. Med 19, 1617–1624. [PubMed: 24216753]

Huang X, Wu J, Spong S, and Sheppard D (1998). The integrin alphav-beta6 is critical for keratinocyte migration on both its known ligand, fibronectin, and on vitronectin. J. Cell Sci 111, 2189–2195. [PubMed: 9664040]

Jiang J, Zheng M, Zhang M, Yang X, Li L, Wang SS, Wu JS, Yu XH, Wu JB, Pang X, et al. (2019). PRRX1 Regulates Cellular Phenotype Plasticity and Dormancy of Head and Neck Squamous Cell Carcinoma Through miR-642b-3p. Neoplasia 21, 216–229. [PubMed: 30622052]

Kueng W, Silber E, and Eppenberger U (1989). Quantification of cells cultured on 96-well plates. Anal. Biochem 182, 16–19. [PubMed: 2604040]

Mariathasan S, Turley SJ, Nickles D, Castiglioni A, Yuen K, Wang Y, Kadel EE III, Koeppen H, Astarita JL, Cubas R, et al. (2018). TGFβ attenuates tumour response to PD-L1 blockade by contributing to exclusion of T cells. Nature 554, 544–548. [PubMed: 29443960]

Melton AC, Bailey-Bucktrout SL, Travis MA, Fife BT, Bluestone JA, and Sheppard D (2010). Expression of αvβ8 integrin on dendritic cells regulates Th17 cell development and experimental autoimmune encephalomyelitis in mice. J. Clin. Invest 120, 4436–4444. [PubMed: 21099117]

Mu D, Cambier S, Fjellbirkeland L, Baron JL, Munger JS, Kawakatsu H, Sheppard D, Broaddus VC, and Nishimura SL (2002). The integrin alpha(v)beta8 mediates epithelial homeostasis through MT1-MMP-dependent activation of TGF-beta1. J. Cell Biol 157, 493–507. [PubMed: 11970960]

Rock JR, Barkauskas CE, Cronce MJ, Xue Y, Harris JR, Liang J, Noble PW, and Hogan BL (2011). Multiple stromal populations contribute to pulmonary fibrosis without evidence for epithelial to mesenchymal transition. Proc. Natl. Acad. Sci. USA 108, E1475–E1483. [PubMed: 22123957]

Sharma P, and Allison JP (2015). The future of immune checkpoint therapy. Science 348, 56–61. [PubMed: 25838373]

Stockis J, Liénart S, Colau D, Collignon A, Nishimura SL, Sheppard D, Coulie PG, and Lucas S (2017). Blocking immunosuppression by human Tregs in vivo with antibodies targeting integrin αVβ8. Proc. Natl. Acad. Sci. USA 114, E10161–E10168. [PubMed: 29109269]

Su G, Hodnett M, Wu N, Atakilit A, Kosinski C, Godzich M, Huang XZ, Kim JK, Frank JA, Matthay MA, et al. (2007). Integrin alphavbeta5 regulates lung vascular permeability and pulmonary endothelial barrier function. Am. J. Respir. Cell Mol. Biol 36, 377–386. [PubMed: 17079779]

Su G, Atakilit A, Li JT, Wu N, Bhattacharya M, Zhu J, Shieh JE, Li E, Chen R, Sun S, et al. (2012). Absence of integrin αvβ3 enhances vascular leak in mice by inhibiting endothelial cortical actin formation. Am. J. Respir. Crit. Care Med 185, 58–66. [PubMed: 21980034]

Takasaka N, Seed RI, Cormier A, Bondesson AJ, Lou J, Elattma A, Ito S, Yanagisawa H, Hashimoto M, Ma R, et al. (2018). Integrin αvβ8-expressing tumor cells evade host immunity by regulating TGF-β activation in immune cells. JCI Insight 3, e122591.

Tauriello DVF, Palomo-Ponce S, Stork D, Berenguer-Llergo A, Badia-Ramentol J, Iglesias M, Sevillano M, Ibiza S, Cañellas A, Hernando-Momblona X, et al. (2018). TGFβ drives immune evasion in genetically reconstituted colon cancer metastasis. Nature 554, 538–543. [PubMed: 29443964]

Thomas DA, and Massagué J (2005). TGF-beta directly targets cytotoxic T cell functions during tumor evasion of immune surveillance. Cancer Cell 8, 369–380. [PubMed: 16286245]

Travis MA, Reizis B, Melton AC, Masteller E, Tang Q, Proctor JM, Wang Y, Bernstein X, Huang X, Reichardt LF, et al. (2007). Loss of integrin alpha(v)beta8 on dendritic cells causes autoimmunity and colitis in mice. Nature 449, 361–365. [PubMed: 17694047]

Wei SC, Levine JH, Cogdill AP, Zhao Y, Anang NAS, Andrews MC, Sharma P, Wang J, Wargo JA, Pe'er D, and Allison JP (2017). Distinct Cellular Mechanisms Underlie Anti-CTLA-4 and Anti-PD-1 Checkpoint Blockade. Cell 170, 1120–1133.e17. [PubMed: 28803728]

Worthington JJ, Kelly A, Smedley C, Bauché D, Campbell S, Marie JC, and Travis MA (2015). Integrin αvβ8-Mediated TGF-β Activation by Effector Regulatory T Cells Is Essential for Suppression of T-Cell-Mediated Inflammation. Immunity 42, 903–915. [PubMed: 25979421]

Wu TC, Xu K, Banchereau R, Marches F, Yu CI, Martinek J, Anguiano E, Pedroza-Gonzalez A, Snipes GJ, O'Shaughnessy J, et al. (2014). Re-programming tumor-infiltrating dendritic cells for CD103+ CD8+ mucosal T-cell differentiation and breast cancer rejection. Cancer Immunol. Res 2, 487–500. [PubMed: 24795361]

Young KH, Baird JR, Savage T, Cottam B, Friedman D, Bambina S, Messenheimer DJ, Fox B, Newell P, Bahjat KS, et al. (2016). Optimizing Timing of Immunotherapy Improves Control of Tumors by Hypofractionated Radiation Therapy. PLoS ONE 11, e0157164. [PubMed: 27281029]

Yumoto K, Eber MR, Wang J, Cackowski FC, Decker AM, Lee E, Nobre AR, Aguirre-Ghiso JA, Jung Y, and Taichman RS (2016). Axl is required for TGF-β2-induced dormancy of prostate cancer cells in the bone marrow. Sci. Rep 6, 36520. [PubMed: 27819283]

Zhang Y, Morgan R, Chen C, Cai Y, Clark E, Khan WN, Shin SU, Cho HM, Al Bayati A, Pimentel A, and Rosenblatt JD (2016). Mammary-tumor-educated B cells acquire LAP/TGF-β and PD-L1 expression and suppress anti-tumor immune responses. Int. Immunol 28, 423–433. [PubMed: 26895637]

Highlights

- ITGB8 on CD4+/CD25+ T cells activates latent TGF-β, causing tumor immunosuppression
- Anti-ITGB8 therapy elicits tumor regression and durable anti-tumor immunity
- CD8+T cells are essential for anti-tumor activity of anti-ITGB8
- Anti-ITGB8 synergizes with multiple immunomodulators in multiple tumor types

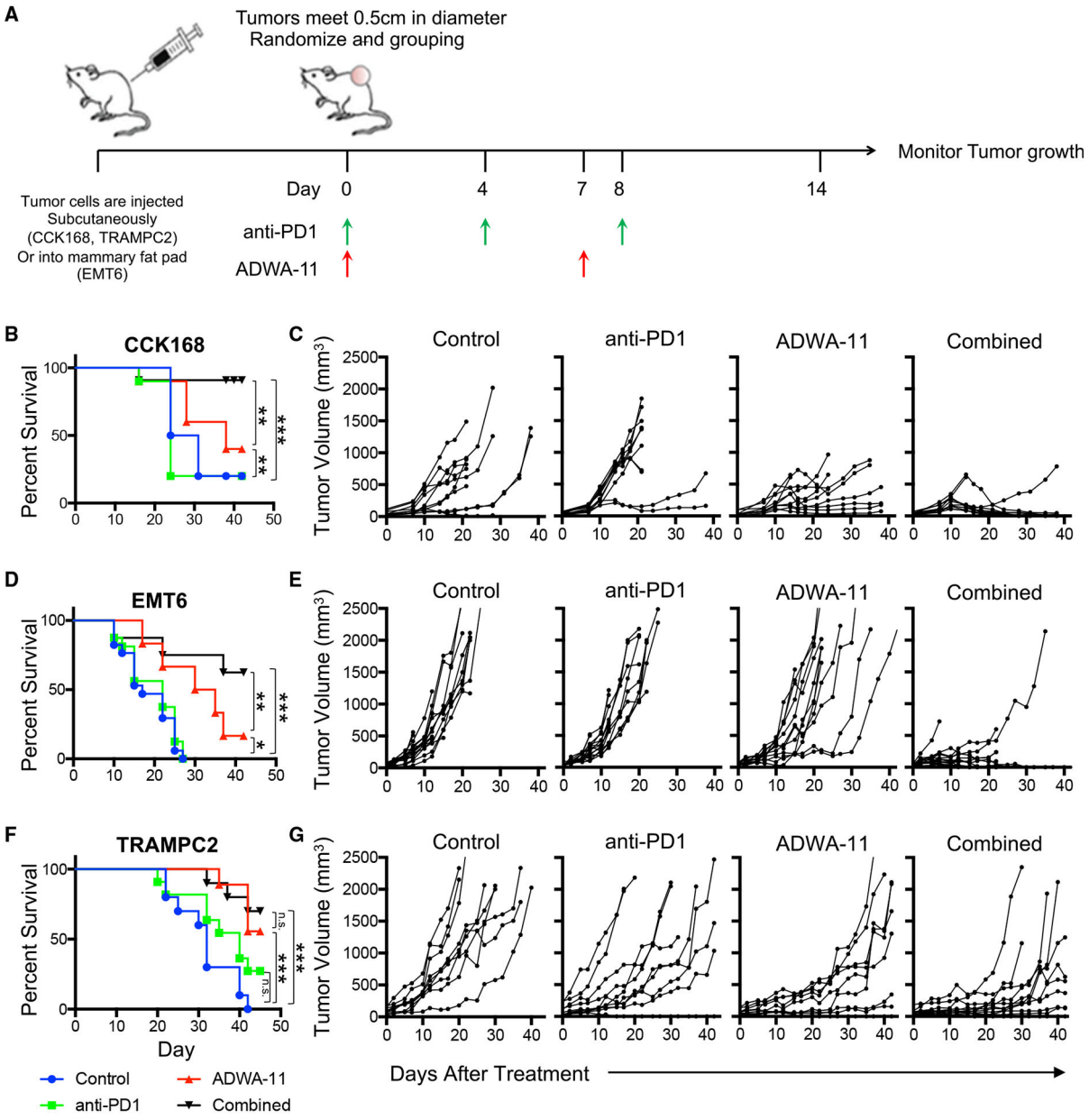

Figure 1. ADWA-11 synergizes with anti-PD-1 to improve survival and decrease tumor size in three solid tumor models

(A) Schematic of multiple tumor models with timeline for injection of tumor cells and antibody injection of 4 treatment groups. Anti-PD-1 was injected intra-peritoneally (i.p.) on days 0, 4, and 8 after the tumor reached the appropriate size for inclusion into the study. ADWA-11 was injected i.p. on days 0 and 7. (B–G) Kaplan-Meier survival curves (B, D, and F) and individual growth curves of tumors were measured every other day for CCK168 (B and C), EMT6 (D and E), and TRAMPC2 (F and G) cells. Mice were euthanized when tumors reached 2,000 mm^3 or more, when extensive tumor ulceration was observed, or at the 45-day endpoint. n = 10–18 in each group. *$p < 0.05$, **$p < 0.01$, ***$p < 0.001$ by log rank Mantel-Cox test.

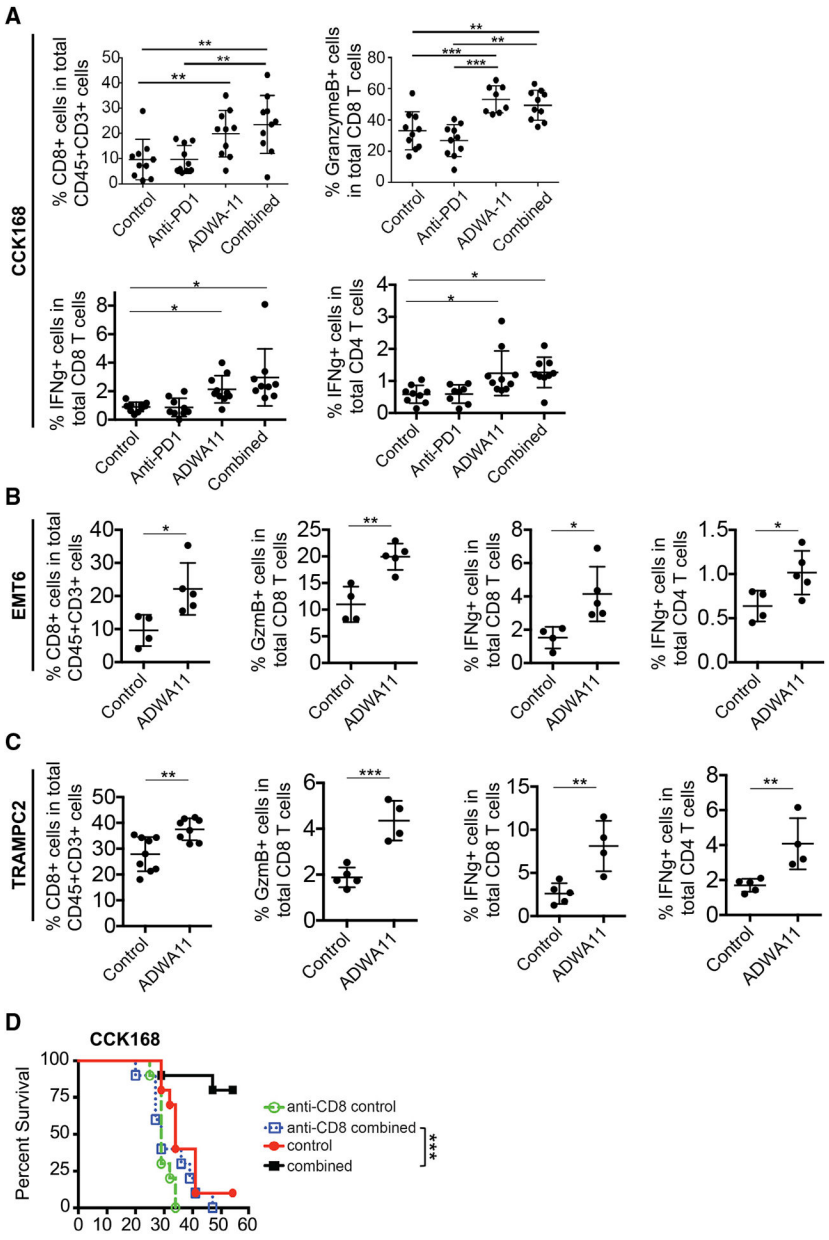

Figure 2. Treatment with ADWA-11 increases accumulation of granzyme B-expressing CD8+ T cells, and depletion of CD8+ T cells abolishes its protective effect

(A) Representative flow cytometry plots showing CD8+ T cells, granzyme B+ CD8+ T cells, and IFNγ+ CD4+ and CD8+ T cells in mice with CCK168 tumors after treatment with control antibodies alone, anti-PD-1, ADWA-11, or combined anti-PD-1 and ADWA-11. n = 10 per group. *p < 0.05, **p < 0.01, ***p < 0.001 by one-way ANOVA. The flow cytometry gating strategy is shown in Figure S2. Data in graphs are mean ± SD; n = 10 per group. *p < 0.05 by one-way ANOVA.

(B and C) Representative flow cytometry plots of EMT6 (B) and TRAMPC2 (C) tumors treated with control and ADWA-11, showing CD8+ T cells, granzyme B+ CD8+ T cells, and IFNγ+ CD4+ and CD8+ T cells. Data in graphs are mean ± SD; n = 5 per group. *p < 0.05, **p < 0.01, ***p < 0.001 by t test.

(D) Survival of mice harboring CCK168 tumors pretreated with an anti-CD8+ depleting antibody or control antibody 1 day prior to initiation of ADWA-11/anti-PD-1 combination therapy. Data are reported as percent survival; n = 10 in each group. ***$p < 0.001$ by log rank Mantel-Cox test.

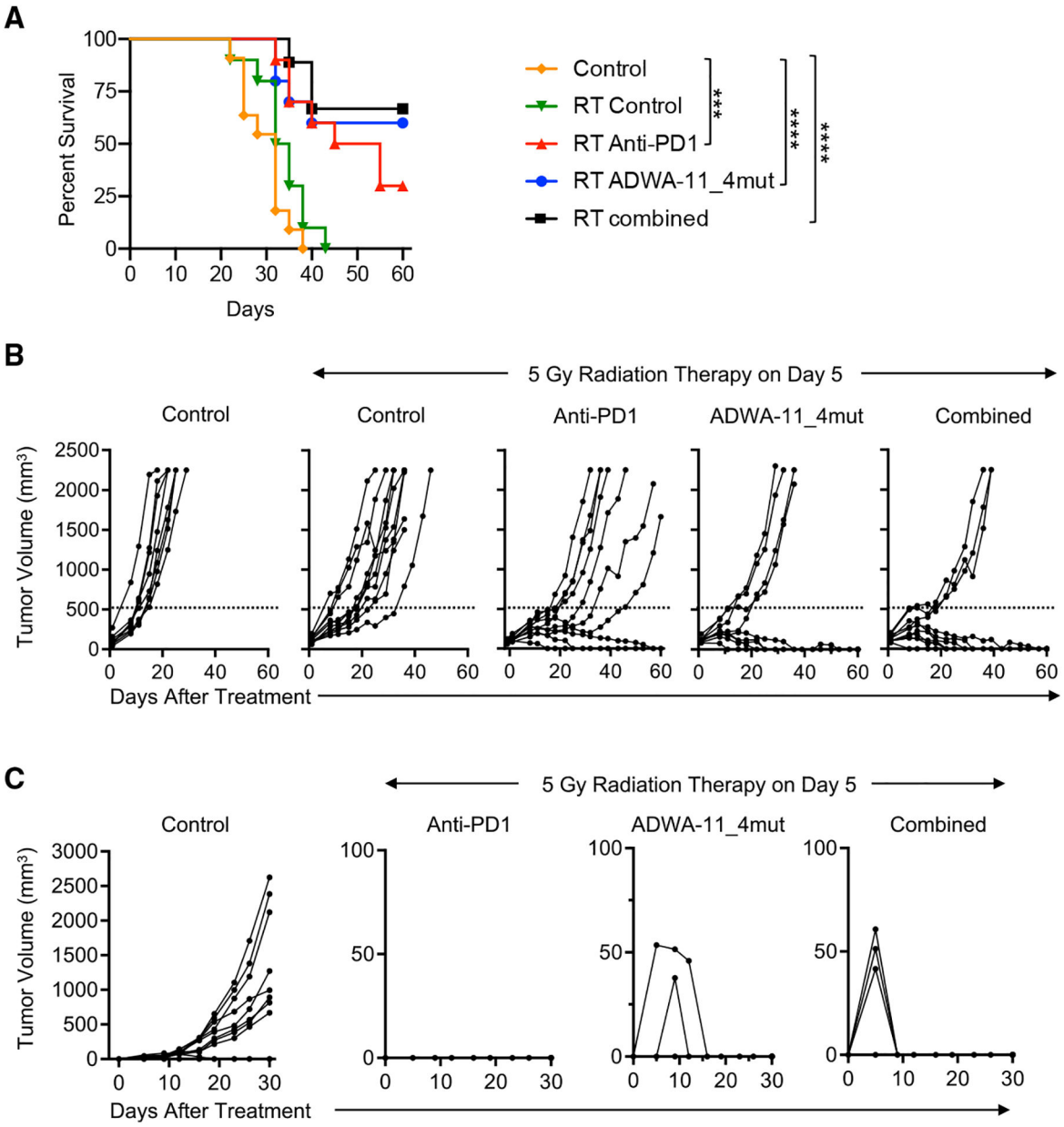

Figure 3. Effectorless ADWA-11_4mut enhances the anti-tumor effects of radiotherapy (RT) and induces long-term anti-tumor immunity in the CT26 colon carcinoma model

(A and B) Survival curves (A) and individual tumor growth curves (B) in mice implanted subcutaneously with CT26 cells treated with isotype control antibodies, anti-PD-1, ADWA-11_4mut, or a combination of anti-PD-1 and ADWA-11_4mut, plus a 5-Gy radiation dose on day 5. One group of mice treated with an isotype control antibody did not receive RT. Data are reported as percent survival; n = 10 in each group. ***$p < 0.001$, ****$p < 0.0001$ by log rank Mantel-Cox test.

(C) Tumor re-challenge in CT26-cured mice that survived 50 days after treatment initiation. Parental CT26 cells were implanted into the flank contralateral to that of the original tumor implantation site of CT26-cured mice 51 days after initiating immunotherapy in combination with radiation therapy. Control mice did not receive radiation and were not exposed

previously to tumor cells. Re-challenged mice were followed for 30 days. Control, n = 10; RT plus anti-PD-1, n = 3; RT plus ADWA-11_mut, n = 5; RT plus ADWA-11_mut and anti-PD-1, n = 7.

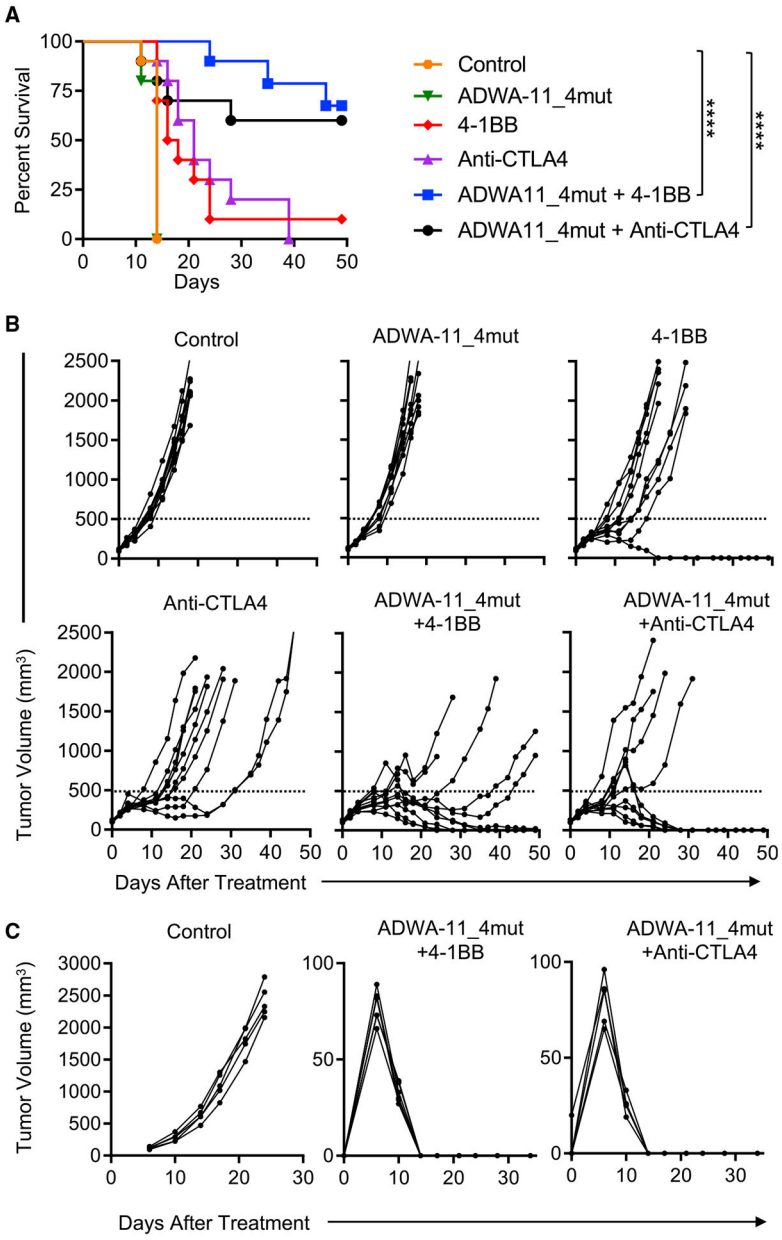

Figure 4. Combination treatment of ADWA-11_4mut with the checkpoint inhibitor anti-CTLA4 or the immune activator 4-1BB also improved survival, inhibited tumor growth, and induced long-term anti-tumor immunity in the EMT6 mammary carcinoma model

(A and B) Survival curves (A) and individual growth curves (B) in mice with orthotopic implantation of EMT6 cells treated with an isotype control antibody, ADWA-11_4mut, 4-1BB, anti-CTLA4, combination of ADWA-11_4mut and 4-1BB, or combination of ADWA-11_4mut and anti-CTLA4. Data are reported as percent survival; n = 10 in each group. ****$p < 0.0001$ by log rank Mantel-Cox test.

(C) Tumor re-challenge in mice that survived 50 days in the EMT6 model after treatment with the combination of ADWA-11_4mut and anti-CTLA4 or the combination of ADWA-11_4mut and 4-1BB. Control mice were not exposed previously to tumor cells. Re-

challenged mice were assessed for 30 days. n = 5 control, n = 6 ADWA-11_4mut + anti-CTLA4, n = 5 ADWA-11_4mut + 4-1BB.

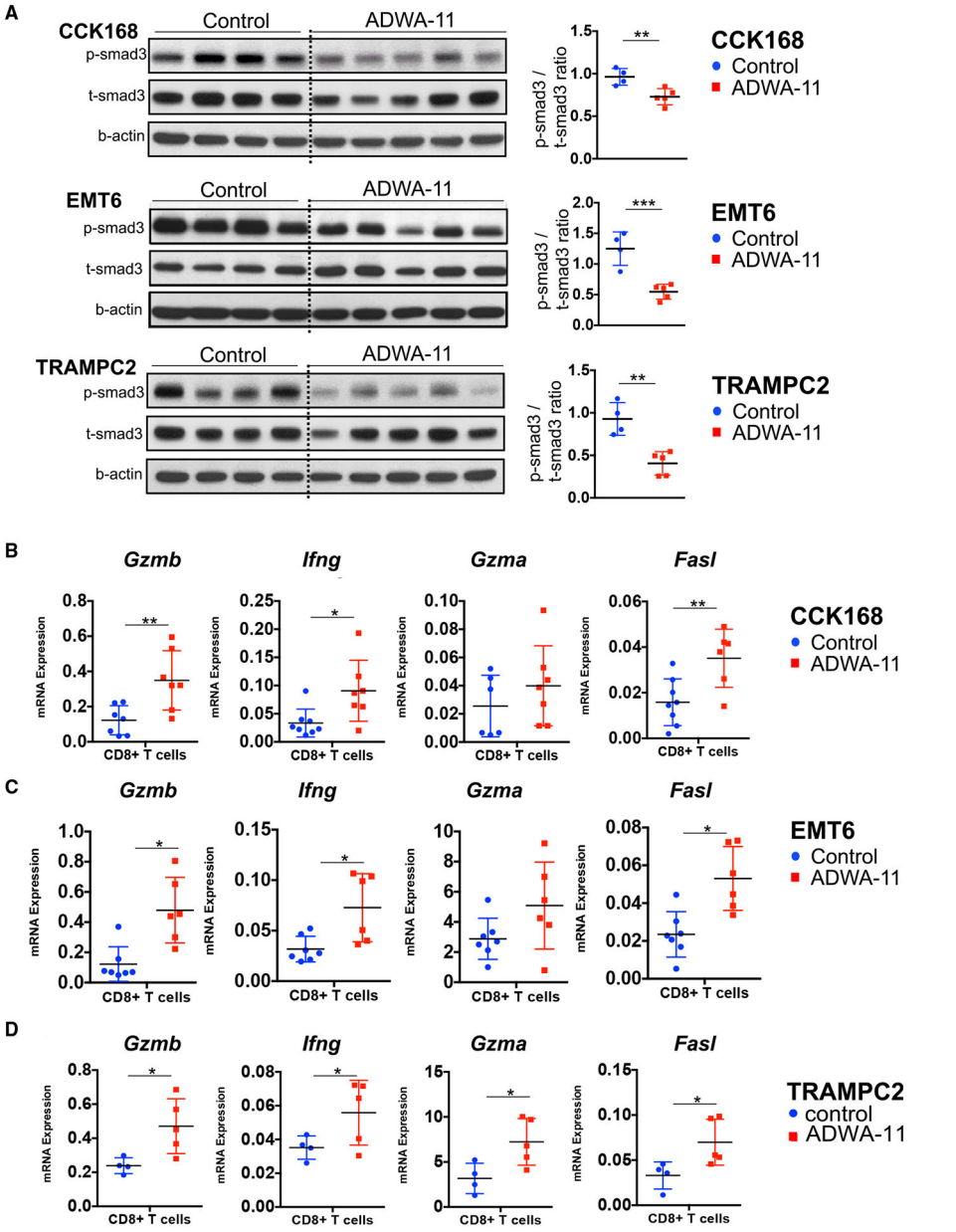

Figure 5. ADWA-11 inhibits TGF-β signaling in tumors and increases expression of genes known to be inhibited by TGF-β in CD8+ T cells

(A) Western blotting for pSMAD3 (and total SMAD3 and β-actin as loading controls) in whole-tumor lysates from CCK168, EMT6, and TRAMPC2 tumors 3 days after ADWA-11 therapy (on days 0 and 7).

(B–D) mRNA expression of a set of genes known to be inhibited by TGF-β (granzyme B, IFN-γ, granzyme A, and Fas ligand) in intratumoral CD8+ T cells from control- or ADWA-11-treated mice harboring CCK168 (B), EMT6 (C), and TRAMPC2 (D) tumors 3 days after ADWA-11 therapy (on days 0 and 7).

Data in graphs are mean ± SD; n = 5–8 per group. *p < 0.05, **p < 0.01 by t test.

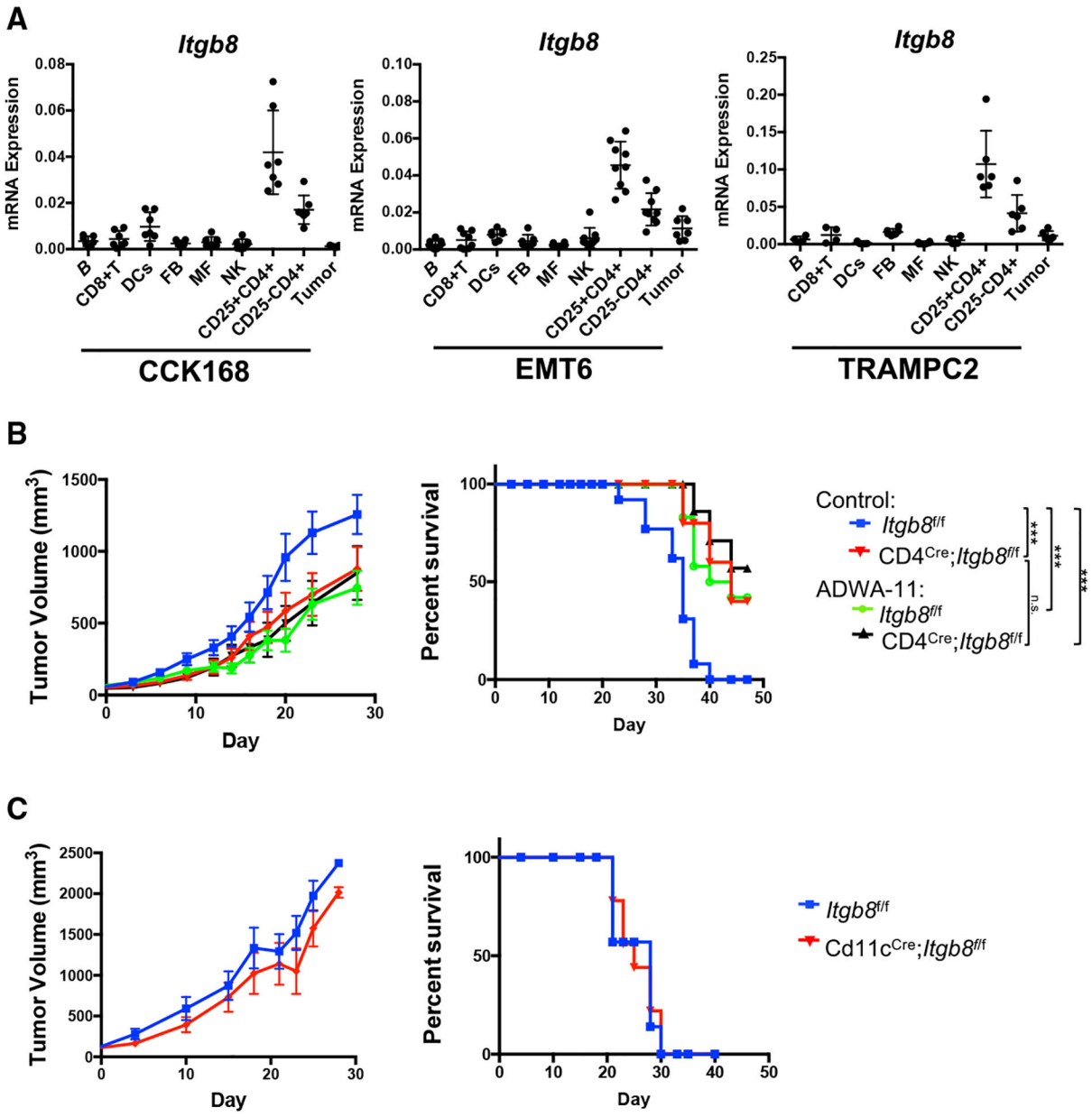

Figure 6. *Itgb8* is most highly expressed in CD25+CD4+ T cells, and deletion of *Itgb8* specifically from T cells but not from CD11c+ cells inhibits *in vivo* growth of TRAMPC2 tumors

(A) Flow cytometry was performed to sort cell populations (Figure S4) from CCK168, EMT6, and TRAMPC2 tumors. mRNA was extracted, and qRT-PCR was performed to detect expression of *Itgb*8 by sorted cell populations. Data in graphs are mean ± SD; n = 6–9 per group.

(B and C) TRAMPC2 tumor cell lines were injected subcutaneously into CD4-Cre;*Itgb8*-f/f (B) or CD11c-Cre;*Itgb8*-f/f mice (C) or *Itgb8*f/f littermate controls After tumors grew to 100–150 mm^3, mice were randomized and separated into two treatment groups for each genotype. Mice were injected i.p. with ADWA-11 or an isotype control antibody on days 0 and 7. Tumor growth was plotted, showing the average volume for each group. Kaplan-Meier survival curves and individual growth curves of tumors were recorded and measured

every other day. Survival curves used a tumor volume of 2,000 mm^3 as cutoff. Mice were euthanized when tumors reached 2,000 mm^3 or more, when extensive tumor ulceration was observed, or at the 45-day endpoint. Data are reported as percent survival; n = 10–18 in each group. ***$p < 0.001$ by log rank Mantel-Cox test.

KEY RESOURCES TABLE

REAGENT or RESOURCE	SOURCE	IDENTIFIER
Antibodies		
Anti- mouse PD1	BioLegend	RMP1–14
Anti-itgavb8	UCSF- Sheppard Lab	ADWA-11
Anti-CD8a	Bio X Cell	53-6.72
ADWA-11 4_mut	Pfizer	N/A
2B8-mlgG_4mut	Pfizer	N/A
Anti-CTLA4	Bio X Cell	9D9
Anti-4-1BB	R and D systems	MAB9371
Anti-avb5	UCSF -Sheppard Lab	ALULA
Anti-avb3	UCSF-Sheppard Lab	Axum-2
Anti-avb6	UCSF Sheppard Lab	10D5
Anti-CD16/30	eBioscience	88-8824
CD45 AF700	Invitrogen	56-0451-80
CD3e BV711	Biolegend	1000241
CD25 BV605	Biolegend	102036
CD4 APC-Cy7	Invitrogend	47-0042-82
NKGG2A/C/E APC	Biolegend	564383
CD8a PE-Cy7	eBioscience	25-0081-81
Granzyme-B PE	eBioscience	12-8898-82
FoxP3 PB-e450	eBioscience	48-5773-82
IFNg BV650	Biolegend	505831
B220 PerCP Cy5.5	eBiosciences	45-0452-80
CD64 FITC	Biolegend	139307
CD11b PE-Cy7	Biolegend	101215
Thy1.2 BV421	Biolegend	105341
Thy1.1 BV421	Biolegend	202529
CD11c BV605	Biolegend	117334
MHCII PE/Dizzle	Biolegend	107648
Annexin V	Biolegend	640909
Rabbit anti-pSMAD3	Abcam	Ab52903
Rabbit anti-total S < AD3	Abcam	Ab40854
Anti-B-actin	Sigma	A5441
Anti-mouse CD8 AF 594 and FITC	Biolegend	Clone 53–6.7
Chemicals, peptides, and recombinant proteins		
Recombinant avb8	R and D Systems	4135-AV-050
TGFb1 Latency associated Peptide	Sheppard Lab	
muFcγRI	R and D Systems	2074-Fc
muFcγRII	R and D Systems	1460-CD
muFcγRIII	R and D Systems	1960-Fc
Experimental models: Cell lines		

REAGENT or RESOURCE	SOURCE	IDENTIFIER
CCK168	Allan Balmain, UCSF	N/A
EMT-6	ATCC	CRL2755
TRAMPC2	ATCC	CRL2731
CT-26	ATCC	CRL-2638
SNB19	ATCC	CRL2219
SW480	Michael Agrez, U Newcastle	N/A
C8-D1A	ATCC	CRL2541
Experimental models: Organisms/strains		
C57BL/6J	Jackson Labs	001800
BALB/c	Charles River	Strain 028
FVB/NJ	Jackson Labs	001800
Itgb8 f/f	Louis Reichardt- UCSF	N/A
B6.Cg-Tg(Cd4-cre)1Cwi/BfluJ	Jackson Labs	022071
Oligonucleotides		
ACTTCTCCTGTCCCTATCTCC	IDT	Itgb8 forward
ATCTGCCACCTTCACACTCC	IDT	Itgb8 reverse
CCACTCTCGACCCTACATGG	IDT	Granzyme B forward
GGCCCCCAAAGTGACATTTATT	IDT	Granzyme B reverse
TCCTCGCCAGACTCGTTTTC	IDT	IFNg forward
GTCTTGGGTCATTGCTGGAAG	IDT	IFNg reverse
TGCTGCCCACCACTGTAACGTG	IDT	Granzyme A forward
GGTAGGTGAAGGATAGCCACCAT	IDT	Granzyme A reverse
TCCGTGAGTTCACCAACCAAG	IDT	FasL forward
GGGGTTCCCTGTTAAATGGG	IDT	FasL reverse
AACCTGCTCCAAAAGTGAACC	IDT	Ms4a1 forward
CCCAGGGTAATATGGAAGAGGC	IDT	Ms4a1 reverse
ATGCGGTGGAACACTTTCTGG	IDT	CD3e forward
GCACGTCAACTCTACACTGGT	IDT	CD3e reverse
TCCTAGCTGTCACTCAAGGGA	IDT	CD4 forward
TCAGAGAACTTCCAGGTGAAGA	IDT	CD4 reverse
CCGTTGACCCGCTTTCTGT	IDT	CD8 forward
CGGCGTCCATTTTCTTTGGAA	IDT	CD8 reverse
GAGGATTTCAGCATCCCAGA	IDT	CD11c forward
CACCTGCTCCTGACACTCAA	IDT	CD11c reverse
GCTCCTCTTAGGGGCCCAT	IDT	Col1a1 forward
CCACGTCTCACCATTGGGG	IDT	Col1a1 reverse
CTTTGGCTATGGGCTTCCAGTC	IDT	F480 forward
GCAAGGAGGACAGAGTTTATCGTG	IDT	F480 reverse
CTCTCTGGGCCTGACTTCTTC	IDT	NKG7 forward
TGTGTCACATGGATATAACCTGC	IDT	NKG7 reverse
ACTCGCATGTTCGCCTACTTCAG	IDT	Foxp3 forward
GGCGGATGGCATTCTTCCAGGT	IDT	Foxp3 reverse

REAGENT or RESOURCE	SOURCE	IDENTIFIER
TGGATTTGGACGCATTGGTC	IDT	Gapdh forward
TTTGCACTGGTACGTGTTGAT	IDT	Gapdh reverse
Software and algorithms		
Graphpad Prism 5.0	Graphpad	N/A
ImageJ	NIH	N/A
FlowJo	Tree Star	N/A